G. M. McNEICE
Associate Professor,
University of Waterloo,
Waterloo, Ontario, Canada

P. V. MARCAL
Professor of Engineering,
Brown University,
Providence, R. I.
Assoc. Mem. ASME

Optimization of Finite Element Grids Based on Minimum Potential Energy

An initial study has been made of a method for optimizing finite element grids. This method is based on the minimum potential energy where the nodal point positions are also treated as independent variables. Necessary conditions have been obtained for the optimized grids. Case studies demonstrate the procedure for a one-dimensional tapered bar under axial load and for a two-dimensional square membrane subjected to a parabolic tensile stress. The optimized grids were observed to give improved stress estimates.

Introduction

THE SELECTION of an element grid is one of the most important decisions in a finite element analysis and yet little work seems to have been done on the subject. To date this selection is based on experience. The literature contains much information on different types of elements and also on the effect of grid refinements [1, 2, 3, 4][1] on the accuracy of solution. In this study we recognize that there are limitations placed on the grid size by the core size and speed of a digital computer. The increasing use of nonlinear analysis which requires an order of magnitude increase in computing time accentuates the need for a coarser grid. Finally, another reason for having an optimized grid is to help the analyst decide where to distribute his nodes in cases where past experience cannot be used as a guide. It is one of the hazards of finite element analysis that a coarse mesh in a high stress gradient region results in an unsafe design.

In this report we shall study the optimization of grids with a fixed number of nodes. The scope of the work does not include the use of optimization algorithms. Rather the equations governing the optimization of grids are developed and a trial-and-error procedure is then used to investigate the implications of the equations.

The principle of minimum potential energy is employed to establish the requirements for a global but discrete minimum. The criterion used for determining the best grid is also based on this minimum. Examples of one- and two-dimensional finite element problems are studied in order to illustrate the method.

Theoretical Considerations

The relationships derived in this section pertain to the displacement model of finite elements although similar formulations involving equilibrium models could be attempted. For the displacement model the principle of minimum potential energy will be used to establish the requirements for the "best" minimum amongst all potential energies associated with solutions based on a predetermined number of specific nodes and elements.

For a compatible model which satisfies the basic criteria of constant stress states and rigid body motion, convergence in energy toward the exact value is known to be monotonic with the degrees of freedom used [5]. The displacements and stresses converge uniformly and in the mean, respectively. It is usually accepted that for this type of model a "better" solution is one that produces a lower potential energy or a higher total strain energy since the latter is always a lower bound to the exact value. If this criterion is applied to the selection of the best mesh distribution as well, then the requirements for the "best" solution can be established in the following manner.

For the displacement model the total potential energy is simply

$$\pi_P = \frac{1}{2}\{u\}^T[K]\{u\} - \{u\}^T\{P\} \tag{1}$$

in which

$\{u\}$—column vector of nodal displacements
$[K]$—square positive definite matrix of stiffness influence coefficients
$\{P\}$—column vector of applied loads

In equation (1) the matrix $[K]$ is a function of nodal coordinates. If $\{P\}$ are energy equivalent loads then they also become functions of the coordinates. Consequently

$$\pi_P = \pi_P(u_i, x_k) \tag{2}$$

[1] Numbers in brackets designate References at end of paper.

Contributed by the Pressure Vessels and Piping Division and presented at the Petroleum Mechanical Engineering Conference with Pressure Vessel and Piping Conference, New Orleans, La., September 17–21, 1972, of THE AMERICAN SOCIETY OF MECHANICAL ENGINEERS. Manuscript received at ASME Headquarters, March 17, 1972. Paper No. 72-PVP-3.

Downloaded From: https://manufacturingscience.asmedigitalcollection.asme.org on 06/28/2019 Terms of Use: http://www.asme.org/about-asme/terms-of-use

Copyright © 1973 by ASME

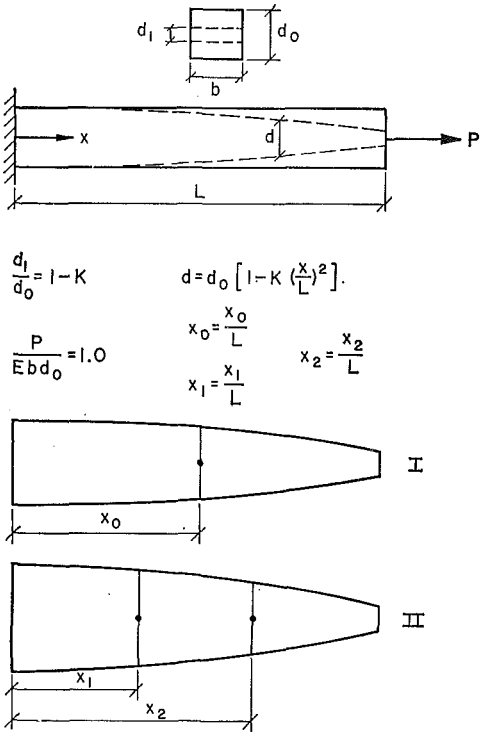

Fig. 1 Tapered bar example

where the subscript denotes node numbers pertaining to the finite element grid. Since the principle of minimum potential energy requires that

$$\delta\pi_P = 0$$

then

$$\frac{\partial\pi_P}{\partial u_i}\,\delta u_i + \frac{\partial\pi_P}{\partial x_k}\,\delta x_k = 0 \tag{4}$$

where the i summation is over the nodal displacements and the k summation is over the nodal coordinates.

Although the displacement u_i is determined at the node having the coordinate x_i, if these parameters are made independent by not prescribing x_k then equation (4) would require that both

$$\frac{\partial\pi_P}{\partial u_i} = 0 \tag{5}$$

and

$$\frac{\partial\pi_P}{\partial x_k} = 0 \tag{6}$$

Applying equation (5) leads to the well known result

$$[K]\{u_i\} - \{P_i\} = 0 \tag{7}$$

The second requirement of equation (6) gives

$$\left(\frac{1}{2}\{u_i\}^T\left[\frac{\partial K}{\partial x_j}\right]\{u_i\} - \{u_i\}^T\left\{\frac{\partial P_i}{\partial x_j}\right\}\right)\frac{\partial x_j}{\partial x_k} = 0 \tag{8}$$

in which $\dfrac{\partial x_j}{\partial x_k} = \delta_{jk}$ *for all interior points and certain boundaries.* For general surface boundaries such as shells x_j can be determined as a function of x_k when $k \neq j$. The matrix $\left\{\dfrac{\partial P_i}{\partial x_j}\right\}$ can be established from the expressions for work equivalent loading on an element.

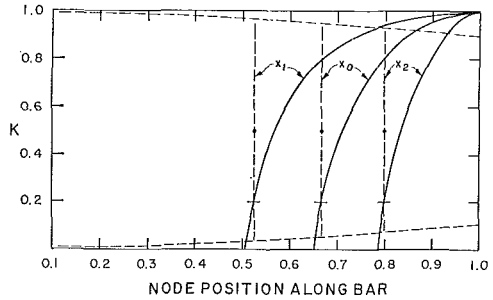

Fig. 2 Effect of taper on optimum grids

Previous finite element solutions satisfy only equation (7) since the nodal coordinates x_k are fixed by the analyst and not allowed to vary.

It is equation (8) which is the subject of this study. If this equation is satisfied simultaneously with equation (7), then the absolute minimum potential energy (in the discrete sense) will be attained. This will give an optimized arrangement of nodes and would constitute an optimum grid for the particular nodes that are allowed to move. For a general finite element problem the complete optimum grid will require that all nodes be allowed to move. The proof that an optimum grid does or does not exist in general or even in specific two- or three-dimensional problems may be difficult to ascertain. An attempt at such a proof is outside the scope of the present study. It is only conjectured, albeit intuitively, on the part of the authors that satisfaction of equations (7) and (8) which gives the best minimum of all potential energy approximations possible from any one discrete model will give the optimum arrangement of the nodal points. The simultaneous satisfaction of (5) and (6) requires the solution of two sets of coupled nonlinear equations. This is of course difficult to achieve and in the following we have adopted an iterative approach to the solution of the problem. Equation (5) is first satisfied through solution of the equilibrium equation (7).

In order to gain some insight concerning the optimization of finite element grids, a simple one-dimensional problem was investigated in which the complete requirements for a minimum were satisfied. The following section discusses the results.

Tapered Axial Bar Example

The tapered bar of Fig. 1 was divided into two and three linear displacement elements and subjected to an axial tensile force. The requirements of equation (7) and (8) were satisfied for various degrees of taper. The optimum locations of the nodes for the full range of taper are illustrated in Fig. 2. This figure shows the position of x_0 for the optimum two element model for various degrees of taper. Also shown are the optimum positions of x_1 and x_2 for the three element model. Superimposed on these results is a sketch of the bar with $\kappa = 0.2$ and the location of x_0, x_1 and x_2 for a two and three element model, respectively. These results establish that at least for the one-dimensional case the optimum was obtained by the iterative procedure. It is interesting to note that, for full taper of $\kappa = 1.0$ in which a stress singularity exists at the tip, the nodes are positioned at the tip. This indicates that a minimum potential energy cannot be obtained and the grids cannot be fully optimized in such cases. However, the process will produce grids that tend toward the minimum and thereby provide better solutions (in energy) at any stage. This will be discussed further in the two-dimensional problem. It is obvious that for $\kappa = 0$ the bar is straight and the node may be positioned anywhere since the exact solution is reproduced in each element (constant stress). We have not investigated this degenerate condition. A final point of interest in Fig. 2 is the fact that the optimum location of x_0 (the nodes of the two element model) lies almost midway between x_1 and x_2, the two nodes

Downloaded From: https://manufacturingscience.asmedigitalcollection.asme.org on 06/28/2019 Terms of Use: http://www.asme.org/about-asme/terms-of-use

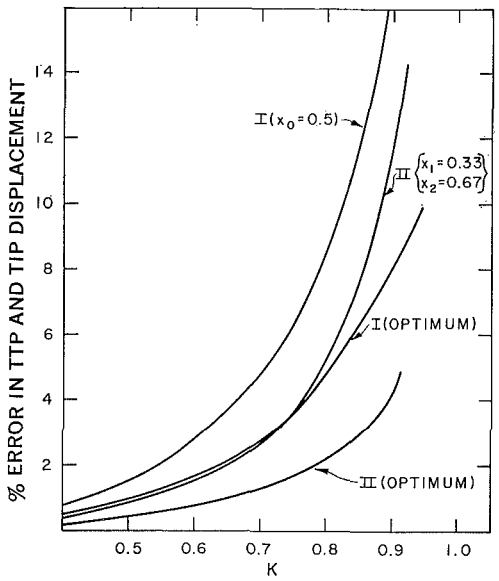

Fig. 3 Percent error from exact solution

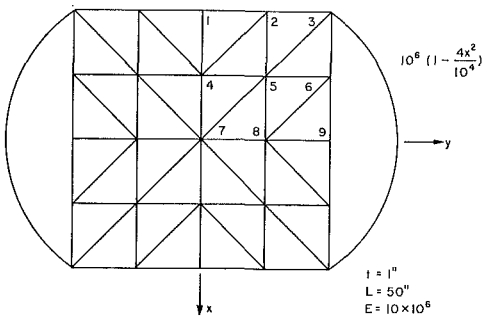

Fig. 4 Original finite element grid

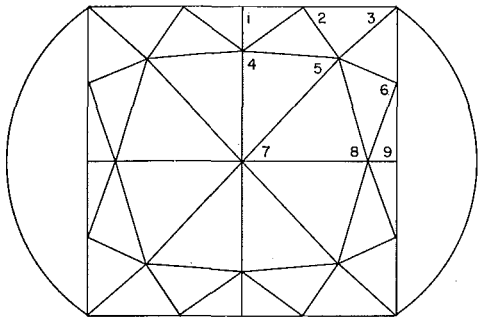

Fig. 5 First modified grid

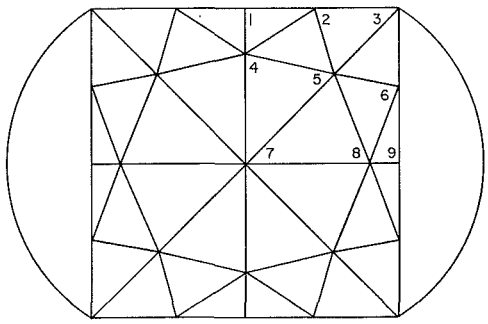

Fig. 6 Second modified grid

of the three element structure. Regardless of taper, no node is found in the widest half length of the bar.

An important consideration in finite element analyses is the discretization error. One measure of this error is a comparison of critical displacements between the discrete model and the exact solution. The practicality of obtaining optimum grids for direct applications will likely be judged upon the degree of reduction in this error. For the tapered bar, Fig. 3 illustrates the percentage error in potential energy and tip displacement for various degrees of taper. In order to illustrate the importance of grid optimization, the optimum grid results are presented along with nonoptimized cases. It is seen that optimized grids reduce the discretization error by 50 percent for taper above $\kappa = 0.4$. Results below this taper are all less than one percent. Fig. 3 also indicates the possibility that an optimized grid can be more accurate than a nonoptimized grid containing more degrees of freedom. A two-dimensional problem will be discussed next.

Plane Stress Square Plate Example

This example was selected only to explore the possibility of applying the above theory to a two-dimensional finite element problem. The square plate (see reference [6]) of Fig. 4, subjected to a parabolic end load was divided into triangular elements as shown. Because of symmetry only one quadrant of the plate was modelled. Only four nodes (2, 4, 5, 8) were allowed to move. Node 6 was maintained fixed in order to reduce the requirements of equation (8) to the following:

$$\frac{1}{2}\{u_i\}^T\left[\frac{\partial K}{\partial x_k}\right]\{u_i\} = 0 \tag{9}$$

For the problem all $\frac{\partial x_j}{\partial x_k} = \delta_{jk}$ and $\frac{\partial P_i}{\partial x_j} = 0$.

This example has not been fully optimized to the extent it can be since it was attempted on an exploratory basis and therefore a computational scheme to solve equations (7) and (8) was not employed. The procedure used was basically manual in the sense that the displacements were determined from

$$[K]\{u_i\} = \{P_i\} \tag{10}$$

for one grid of x_k's and substituted into

$$\frac{1}{2}\{u_i\}^T\left[\frac{\partial K}{\partial x_k}\right]\{u_i\} = \{\epsilon_k\} \tag{11}$$

to give a vector of so called "error" terms. Appendix A contains the matrix algebra in equation (11) for the linear displacement triangle. The error terms are simply

$$\{\epsilon_k\} = \left\{\frac{\partial \pi_P}{\partial x_k}\right\} \tag{12}$$

and therefore the sign of each ϵ_k establishes the direction in which node k should move. The nodes were moved in these indicated directions by an amount based on the relative magnitudes of the $\{\epsilon_k\}$ and the total distance available to a neighboring node position. All the nodes were moved initially resulting in the MOD 1 grid of Fig. 5. $\{\epsilon_k\}$ were recalculated and the process continued with only certain nodes being moved. The third and the seventh grids are shown in Figs. 6 and 7, respectively.

The history of modifications and values of the errors are presented in Table 1. The procedure used here is based on trial and error but the results are rather encouraging.

Downloaded From: http://manufacturingscience.asmedigitalcollection.asme.org on 06/28/2019 Terms of Use: http://www.asme.org/about-asme/terms-of-use

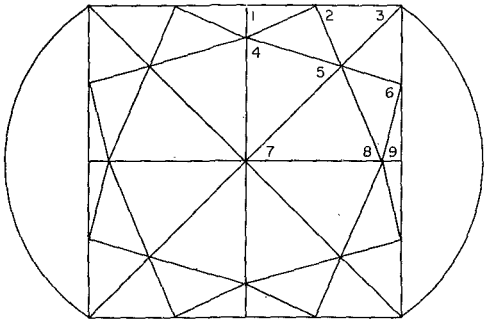

Fig. 7 Final modified grid

Table 1 History of modifications

NODE	ITEM	ORIGINAL	MOD 1	MOD 2	MOD 3	MOD 4	MOD 5	MOD 6	MOD 7
2	y_2	25.00	20.00	22.50	23.00	23.00	23.00	23.00	23.00
4	x_4	-25.00	-35.25	-35.25	-35.75	-35.75	-35.75	-35.75	-39.00
5	x_5	-25.00	-34.25	-29.63	-30.00	-30.00	-30.00	-30.00	-30.00
	y_5	25.00	31.00	28.00	30.00	30.00	30.00	30.00	30.00
8	y_8	25.00	41.25	41.25	41.25	45.00	43.25	43.50	43.50
2	$\frac{\partial \pi_p}{\partial y_2}$	19.67*	-18.18	9.43	5.66	5.75	5.72	5.73	2.67
4	$\frac{\partial \pi_p}{\partial x_4}$	20.54	0.92	8.22	5.38	5.44	5.43	5.43	-0.51
5	$\frac{\partial \pi_p}{\partial x_5}$	37.03	-34.33	5.64	3.16	-4.18	-0.86	-1.34	-1.13
	$\frac{\partial \pi_p}{\partial y_5}$	-24.01	24.09	-16.02	-4.49	-4.81	-4.48	-4.50	-0.66
8	$\frac{\partial \pi_p}{\partial y_8}$	-64.89	-0.40	-18.30	-17.20	11.40	-2.76	-0.81	-0.83
Strain Energy		237.2158	240.3148	240.5846	240.6688	240.6984	240.7134	240.7144	240.7474

* Multiply all values by 10^3.

Although the seventh modification has error terms far from zero, they are considerably smaller than the original values. They show consistently that reductions in ϵ_k lead to a better minimum potential energy (or higher strain energy) and give better stresses as illustrated in Table 2.

It is interesting to note that the last grid produced triangles that tend toward an equilateral shape. Past experience has established that such triangles give improved results. Certainly, the final grid is far removed from the original (a common grid for plates) and one that few if any analysts would select initially.

The authors consider this example as a stimulus with respect to the ideas outlined above and are currently researching methods of automating the procedure.

Conclusion

The necessary conditions for an absolute (discrete) minimum potential energy in a compatible displacement model of finite elements has been stated. An interpretation has been given when the number of nodes used is limited and when the nodal geometry is allowed to change. When applied to a one-dimensional problem the results produced optimum grids when they existed. The two-dimensional problem served to illustrate that the criterion assumed for producing better solutions was correct. Although an optimum grid was not obtained for lack of an automated computer algorithm, the results are sufficiently encouraging to warrant additional study.

Acknowledgments

The authors are indebted to Prof. P. R. Paslay for suggesting the one-dimensional example and to Prof. R. H. Plaut for his assistance in the computation and his encouragement through out this study.

Table 2 Normal stress ($\sigma_y \times 10^{-5}$)

NODE	ORIGINAL	MOD 1	MOD 2	MOD 7	EXACT
1	5.10(24)*	5.26(28)	4.88(19)	4.81(17)	4.11
7	4.38(-14)	6.00(-30)	7.51(-12.5)	7.50(-12.7)	8.59
6	7.44(-0.8)	7.27(-3)	7.40(-1.3)	7.43(-1)	7.50
9	8.34(-16.6)	9.15(-8.5)	9.10(-9)	9.24(-7.6)	10.00

* (%) error

References

1 Proceedings of the Second Conference on Matrix Methods in Structural Mechanics, Wright-Patterson Air Force Base, Dayton, Ohio, Oct. 1968.

2 Gallagher, R. H., "Analysis of Plate and Shell Structures," Application of Finite Element Methods in Civil Engineering, A.S.C.E.—Vanderbilt University Symposium, Nashville, Tennessee, Nov. 1969.

3 Felippa, C. A., "Refined Finite Element Analysis of Linear and Nonlinear Structures," PhD thesis, Dept. of Civil Engineering, University of California, Berkeley, California, 1966.

4 "Finite Element Methods in Stress Analysis," *TAPIR*, Trondheim, Norway, 1969.

5 Key, S. W., "A Convergence Investigation of the Direct Stiffness Method," PhD thesis, University of Washington, 1966.

6 Cowper, G. R., Lindberg, G. M., and Olson, M. D., "A Shallow Shell Element of Triangular Shape," *International Journal of Solids and Structures*, Vol. 6, 1970, pp. 1133–1156.

APPENDIX

Derivation of $\{\epsilon_k\}$ for the Constant Stress Triangle

The constant stress triangle is derived using the linear displacement polynomials

$$u = a_1 + a_2x + a_3y$$
$$v = a_4 + a_5x + a_6y \tag{12}$$

or in matrix form

$$u = \{R\}^T\{a\} \tag{13}$$

Substituting nodal coordinates x_k in matrix R leads to the nodal displacement matrix of the element,

$$\{u\} = [C]\{a\} \tag{14}$$

such that the general displacement interpolation becomes

$$u = \{R\}^T[C]^{-1}\{u\} \tag{15}$$

Since the strain displacement relations are simply derivatives of equation (15), the strains are

$$\{\epsilon\} = \{B\}^T[C]^{-1}\{u\} \tag{16}$$

The stresses are then

$$\{\sigma\} = [D]\{\epsilon\} \tag{17}$$

Thus far only matrix $[C]$ is a function of nodal coordinates.

The potential energy is then

$$\pi_p = \frac{1}{2}\{u\}^T[C]^{-T}\int_V \{B\}^T D\{B\}dV[C]^{-1}\{u\} - \{u\}^T\{F\} \tag{18}$$

For the constant strain triangle the integrand is a constant scalar quantity and equation (18) reduces to

$$\pi_p = \frac{1}{2}\{u\}^T[C]^{-T}\{B\}^T[D]\{B\}[C]^{-1}At\{u\} - \{u\}^T\{F\} \tag{19}$$

$$= \frac{1}{2}\{u\}^T[k]\{u\} - \{u\}^T\{F\} \tag{20}$$

Recalling equation (9) as

Downloaded From: https://manufacturingscience.asmedigitalcollection.asme.org on 06/28/2019 Terms of Use: http://www.asme.org/about-asme/terms-of-use

$$\{u\}^T \left[\frac{\partial k}{\partial x_k}\right] \{u\} = 0 \tag{21}$$

it is evident that by differentiating by parts

$$\left[\frac{\partial k}{\partial x_k}\right] = \frac{1}{A}[k]\frac{\partial A}{\partial x_k} - [C]^{-T}\left[\frac{\partial C}{\partial x_k}\right]^T [k] - [k]\left[\frac{\partial C}{\partial x_k}\right][C]^{-1} \tag{22}$$

in which A is the area and function of x_k. Thickness t is in equation (19) and is of course in $[k]$. Note that the last term in equation (22) is the transpose of the second term and also that the stress strain relation D and the displacement to strain transformation matrix $\{B\}$ are independent of the nodal position x_k.

For a typical triangle with nodes l, m, and n the area is given by

$$\tfrac{1}{2} \det. \begin{bmatrix} 1 & x_l & Y_l \\ 1 & x_m & Y_m \\ 1 & x_n & Y_n \end{bmatrix} \tag{23}$$

and the $[C]$ matrix is simply

$$\begin{bmatrix} 1 & x_l & Y_l & 0 & 0 & 0 \\ 1 & x_m & Y_m & 0 & 0 & 0 \\ 1 & x_n & Y_n & 0 & 0 & 0 \\ 0 & 0 & 0 & 1 & x_l & Y_l \\ 0 & 0 & 0 & 1 & x_m & x_m \\ 0 & 0 & 0 & 1 & x_n & x_n \end{bmatrix}$$

Consequently equation (22) is a trivial matrix calculation.

For elements with other than a constant stress equation (11) and for a general case equation (8) will have to be calculated numerically. However, even in the most general case, all calculations can be performed on a single element at a time basis. This follows from the fact that the total potential energy for a compatible finite element model consists of the sum of individual element contributions.

Downloaded From: https://manufacturingscience.asmedigitalcollection.asme.org on 06/28/2019 Terms of Use: http://www.asme.org/about-asme/terms-of-use